J. Appl. Comput. Mech., 7(2) (2021) 646-654
DOI: 10.22055/JACM.2020.35475.2668

ISSN: 2383-4536
jacm.scu.ac.ir

Shahid Chamran University of Ahvaz

Journal of Applied and Computational Mechanics

Research Paper

Robust P-H_∞ Integrated Controller for Flexible Link Manipulator System in the Presence of Disturbance

Esmail Ali Alandoli[1], T. S. Lee[1], Chu A. My[2], Marwan Qaid Mohammed[1]

[1] Faculty of Engineering and Technology, Multimedia University, 75450 Bukit Beruang, Melaka, Malaysia

[2] Department of Special Robotics and Mechatronics, Le Quy Don Technical University, 236 Hoang Quoc Viet, Hanoi, Vietnam

Received October 21 2020; Revised December 02 2020; Accepted for publication December 03 2020.
Corresponding author: E.A. Alandoli (alandolie@yahoo.com)

Abstract. Flexible link manipulators have recently high attention in research due to the numerous advantages over traditional manipulators. However, flexible link manipulators still have critical problem of less position accuracy due to the tip vibration. Thus, this research contributes by developing a robust P-H_∞ integrated controller for a flexible link manipulator (FLM). The P-H_∞ integrated controller is a combination of Proportional (P) controller and H_∞ controller which helps of possession several advantages such as optimal position tracking, effective vibration repression, and robust to reject disturbances. The proposed P-H_∞ integrated controller has been simulated to control the FLM system using MATLAB/Simulink toolbox. The results have demonstrated satisfactory performance of the proposed P-H_∞ integrated controller in terms of position tracking, vibration repression, and disturbance rejection.

Keywords: Flexible link manipulator, P-H_∞ integrated controller, Position tracking, Vibration suppression, Disturbance rejection.

1. Introduction

Flexible link manipulators (FLMs) were basically manufactured to possess various features such as lightweight, carry a high payload, reach to a wider workspace [1,2]. Some operation can be performed with less energy and faster responses such as moving and manipulate objects by utilizing FLMs in robots instead of rigid link manipulators (RLMs) [3]. Traditionally, robotic manipulators are manufactured to be stiff, rigid and heavy which have good position accuracy as there are no tip vibration or deflection [4,5]. However, such robots are slow response and have the disadvantage of high energy consumption due to the demand of using big size actuators [6]. In contrast, FLMs can be manipulated using small size actuators which are advantageous over RLMs and leads to various features such as less energy consumption, cheap cost and faster speed response [7-9]. Due to the numerous advantages, there is a high attention on FLMs and have a wider range of applications such as medical robots, space robots [10-12], also encouraged to be used in military activities and sectors of agriculture and homecare [9]. Furthermore, FLMs are safer to execute tasks and operations near to workers than RLMs [13].

Several control methods have been proposed and designed to control FLMs and suppress its vibration [14]. A comparative study of PID controller and state feedback controller was implemented for flexible joint manipulator (FJM) in ref. [15], the results show that the state feedback controller has faster response of position tracking (PT), but it has larger overshoot and tip vibration which indicate that the proposed controllers need improvement for better effectiveness of vibration suppression (VS). A neural network (NN) and PID integrated controller was developed in [16], the hybrid NN/PID controller demonstrated improved performance than PID in terms of PT and VS. The more the hidden layers of the NN the better performance, but the long time of the network training is the main drawback. Another integration is a PD controller with a PID controller was studied for the purpose of PT and tip VS in [17], the performance of the integrated PD/PID controller was satisfactory in terms of PT but the tip vibration takes a long time to be eliminated.

Fuzzy logic controller (FLC) was proposed in [14] to control a FJM in terms of PT and reduction of the residual vibration, the performance of the proposed FLC was not satisfactory and there was a difficulty of obtaining the optimal tuned membership functions and rules. An improved FLCs were proposed in ref. [18] and [19] by the optimization of modified invasive weed optimization (MIWO) to enhance the PT and the effectiveness of the tip VS for a FLM system, but there was no significant improvement. Smart materials of Piezoelectric (PZT) actuators were used for active VS of a FLM system in [20] in conjunction with fuzzy sliding mode and linear quadratic regulator (LQR) controllers. Another research in [21] studied the optimal placement of PZT actuators along a FLM for VS with employing a fuzzy self-tuning PID controller. The active vibration can be effectively reduced by increasing the number of the PZT actuators, but it leads to increasing the link's weight and influence its flexibility [22]. Another issue of utilizing the PZT is the difficulty of obtaining the optimal position along the link [20].

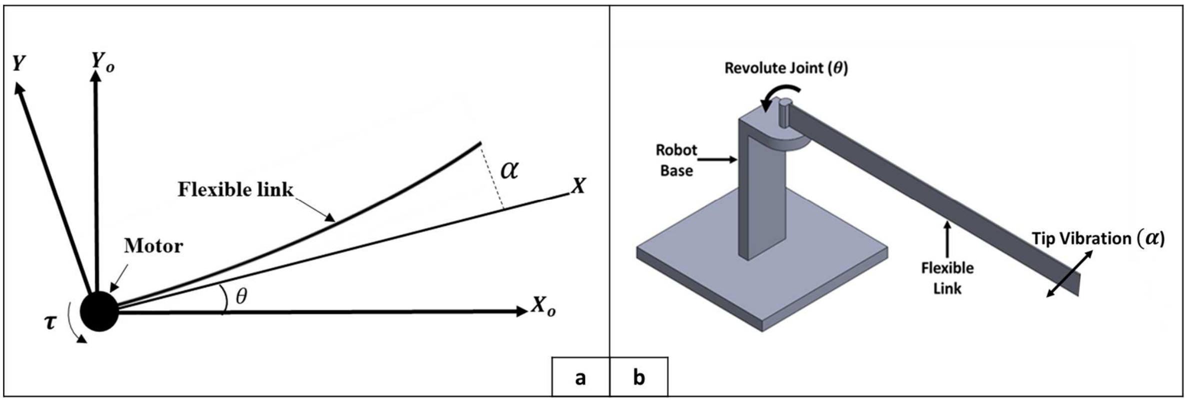

Fig. 1. FLM system: a) schematic diagram. b) Assembly of the system designed by the Inventor software.

A comparison study of LQG controller and H_∞ controller for control a FLM was reported in [23], the comparison showed that the LQG performance is better than the H_∞ performance for the PT of the FLM system. A hybrid controller of H_2/H_∞ was proposed in [1] based on linear matrix inequality (LMI) optimization for the aim of the motion control and the tip VS of a FLM. Also in [24], H_∞ controller was developed using loop shaping method to control FJM, the controller had satisfactory performance for the PT, the weighing function is difficult and tedious to be optimally selected because it is based on trial and error. LQR controller and PID controller were compared for the PT and tip VS of a FLM, the LQR demonstrated better performance than the PID in both PT and tip VS. However, the tip vibration needs to be more reduced and eliminated in shorter time [7]. A combination of PID/LQR controller was developed in [25], the hybrid PID/LQR controller showed better effectiveness for the VS than the PID controller alone. Another comparison of LQR controller with the pole placement controller was studied in [26]. Sliding mode controller was developed for the PT and tip VS of a FLM, a PT error is noticed in the controller response, another disadvantage is the chattering phenomenon which negatively influences the performance and it is essential to be removed [27]. Several modelling methods of FLMs are critically reviewed in [28], and in ref. [29] many control techniques for FLMs are critically and deeply discussed.

There are many control techniques has been proposed and developed to control FLMs. However, there is still a wide scope for contribution in terms of control FLMs. This is because the tip vibration of FLMs has not been totally eliminated by the existing controllers [14]. Due to the tip vibration of FLMs that caused by the flexibility, a controller must carry out two different tasks: PT and VS which imposes the control difficulty of FLMs to double compared to control RLMs [30]. Thus, the control techniques that have used to control RLMs cannot be used to control FLMs and there is a need to particular robust controllers to get rid of the issue of vibration and have optimal PT performance [3].

The objective of this research is to propose and design a robust P-H_∞ integrated controller for optimal PT and effective VS of the FLM system to overcome the problem of less position accuracy and vibration of FLMs. The remaining of the paper is organized as follows: (i) Dynamic model, (ii) controller design, (iii) MATLAB simulation results, (iv) conclusion and future work.

2. Dynamic Model

The FLM system includes of a DC motor and the flexible link. Fig. 1 shows the FLM system. The hub angular position is expressed by θ and α presents the tip vibration of the FLM which.

The mathematical model of the FLM is expressed in eq. (1) and eq. (2). The state space form of the dynamic model has been used for control in several researches [31-34].

$$\begin{bmatrix}\dot{\theta}\\ \dot{\alpha}\\ \ddot{\theta}\\ \ddot{\alpha}\end{bmatrix}=\begin{bmatrix}0 & 0 & 1 & 0\\ 0 & 0 & 0 & 1\\ 0 & \dfrac{k_s}{J_{eq}} & -\dfrac{\eta_m\eta_g k_t k_m k_g^2+B_{eq}R_m}{J_{eq}R_m} & 0\\ 0 & \dfrac{-k_s(J_{eq}+J_{\text{link}})}{J_{eq}J_{\text{link}}} & \dfrac{\eta_m\eta_g k_t k_m k_g^2+B_{eq}R_m}{J_{eq}R_m} & 0\end{bmatrix}\begin{bmatrix}\theta\\ \alpha\\ \dot{\theta}\\ \dot{\alpha}\end{bmatrix}+\begin{bmatrix}0\\ 0\\ \dfrac{\eta_m\eta_g k_t k_g}{J_{eq}R_m}\\ \dfrac{-\eta_m\eta_g k_t k_g}{J_{eq}R_m}\end{bmatrix}u \tag{1}$$

$$Y=\begin{bmatrix}1 & 0 & 0 & 0\\ 0 & 1 & 0 & 0\end{bmatrix}X \tag{2}$$

The system identifications and numerical values are expressed in Table (1).

3. Controller Design

The proposed controller in this research is a robust controller to control FLM system based on P controller and H_∞ controller. P controller is integrated with H_∞ controller to work as a new control technique. The proposed controller in this research has the feature of the capability of P controller to enhance the system response and it is easy of tuning, also the H_∞ controller has the effective capability to suppress the tip vibration and to reject disturbances.

3.1 H_∞ Controller Design

A generalized plant $G(s)$ and a robust controller $K(s)$ are the two components of the H_∞ control system as shown in Fig. 2. The generalized plant $G(s)$ is explained by eq. (3) and eq. (4).

Table 1. System numerical values

Symbol	Description	Value
B_{eq}	Damping coefficient of high gear viscous	0.004 (N.m.s/rad)
J_{eq}	Equivalent high gear moment of inertia without external load	0.00208 kg.m^2
η_m	Efficiency of motor	0.69
η_g	Efficiency of gearbox	0.90
k_m	Back-emf constant	0.00768 (V.s/rad)
k_g	High gear ratio	14:5
k_t	Motor torque constant	0.00768 Nm/A
R_m	Motor armature resistance	2.6 Ω
J_{link}	Moment of inertia of the link	0.0549 kg/m
k_s	Stiffness constant	0.0172 N.m/rad

$$\begin{aligned} \dot{x} &= Ax + B_1\omega + B_2u \\ z &= C_1x + D_{11}\omega + D_{12}u \\ y &= C_2x + D_{21}\omega + D_{22}u \end{aligned} \tag{3}$$

$$\begin{bmatrix} \dot{x} \\ z \\ y \end{bmatrix} = \begin{bmatrix} A & B_1 & B_2 \\ C_1 & D_{11} & D_{12} \\ C_2 & D_{21} & D_{22} \end{bmatrix} \begin{bmatrix} x \\ \omega \\ u \end{bmatrix} \tag{4}$$

where x is the state variable, z is the evaluation signal, y is the measured signal, ω is the exogenous input signal, u is the control input signal, A is the state matrix, B is the input matrix, and C is the output matrix.

The standard H_∞ controller is formulated in [35] as in eq. (5) to eq. (7). LFT is a linear fractional transformation.

$$K(s) = LFT\{K_C, Q\} \tag{5}$$

where:

$$K_c = \left[\begin{array}{c|cc} \hat{A} & -ZL & Z\hat{B}_2(D_{12}^T D_{12})^{-1/2} \\ \hline F & 0 & (D_{12}^T D_{12})^{-1/2} \\ -(D_{21}D_{21}^T)^{-1/2}\hat{C}_2 & (D_{21}D_{21}^T)^{-1/2} & 0 \end{array}\right] \tag{6}$$

$$\begin{aligned} \hat{A} &= A + B_1B_1^T X_\infty + B_2F + ZL\hat{C}_2 \\ \hat{B}_2 &= B_2 + Y_\infty C_1^T D_{12} \\ \hat{C}_2 &= C_2 + D_{21}B_1^T X_\infty \\ F &= -\hat{D}_{12}C_1 - (D_{12}^T D_{12})^{-1} B_2^T X_\infty \\ L &= -B_1\hat{D}_{21} - Y_\infty C_2^T (D_{21}D_{21}^T)^{-1} \\ Z &= (I - Y_\infty X_\infty)^{-1} \\ \hat{D}_{21} &= D_{21}^T (D_{21}D_{21}^T)^{-1} \\ \hat{D}_{12} &= D_{12}^T (D_{12}D_{12}^T)^{-1} \end{aligned} \tag{7}$$

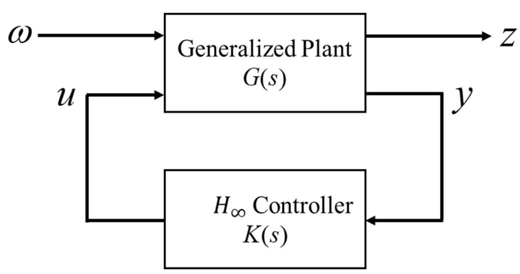

Fig. 2. H_∞ controller diagram

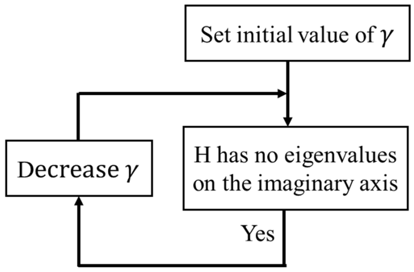

Fig. 3. Calculating *H*∞ norm flow chart

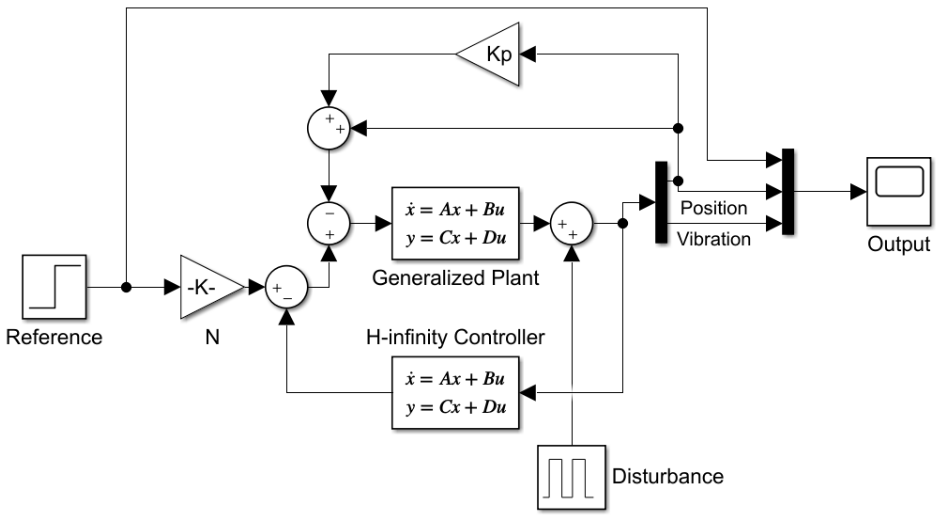

Fig. 4. *P-H*∞ integrated controller scheme

Q(s) is a free parameter and can be neglected if it does not influence the system performance.

The first step of design a standard *H*∞ controller is to find the *H*∞ norm γ which can be computed from the Hamiltonian matrix presented in eq. (8). Fig. 3 shows the flow chart which is used to find the suitable value of γ based on trial and error.

$$H = \begin{bmatrix} A & \frac{BB^T}{\gamma^2} \\ -CC^T & -A^T \end{bmatrix} \tag{8}$$

The optimal value of γ which is found by the interactions in Fig.3 is to be used to solve the Algebraic Riccati Equations (AREs) shown in eq. (9) and eq. (10) to have the stable solution for $X_\infty \geq 0$ and $Y_\infty \geq 0$ respectively [34].

$$A^T X_\infty + X_\infty A + X_\infty(\gamma^{-2}B_1B_2^T - B_2B_2^T)X_\infty + C_1^TC_1 = 0 \tag{9}$$

$$AY_\infty + Y_\infty A^T + Y_\infty(\gamma^{-2}C_1^TC_1 - C_2^TC_2)Y_\infty + B_1B_1{}^T = 0 \tag{10}$$

The following matrix in in eq. (11) is the designed *H*∞ controller which is obtained based on the pervious explanation.

$$K_c = \left[\begin{array}{cccc|cc} 0.00 & 1.9150 & 1.00 & 0.00 & -1.9150 & -3.0590 \\ 0.00 & -41.0830 & 0.00 & 1.00 & 41.0830 & -2.8510 \\ -123.465 & 671.995 & -38.683 & -1.844 & -0.465 & 61.761 \\ 123.465 & -1279.57 & 38.683 & 1.844 & -0.659 & -61.689 \\ \hline -2 & -0.025 & -0.057 & -0.030 & 0 & 1 \\ 0 & -1 & 0 & 0 & 1 & 0 \end{array}\right] \tag{11}$$

3.2 P Controller Design

P controller is tuned to be integrated with *H*∞ controller as shown in Fig. 4, where N is a gain to enhance the system steady state error, e_{ss} , *P* controller is manually tuned as it is easy to be manually tuned and this is an advantage in terms of design simplicity. The proportional gain, K_p, is manually selected to be 50 after many trails in order to be used as the optimal gain and *N* is determined based on error and trial to be 52 as presented in Table (2).

Table 2. Analysis of transient response for closed loop response

$T_r(s)$	$T_s(s)$	OS(%)	$e_{ss}(rad)$
1.1192	2.0359	0.00	1×10^{-4}

Table 3. Analysis of tip vibration for closed loop response

Largest peak to peak (rad)	Stable Time (s)
0.06129	0.6

4. Results and Discussion

The results of the FLM system are deeply discussed in this section for the closed loop response without controller and once the system is controlled by the proposed *P-H*∞ integrated controller.

4.1 Closed Loop Performance without Controller

The closed loop response of the FLM system without a controller is presented by the dash-dot blue line shown in Fig. 5 for the PT response and the solid red line presents the tip vibration. The PT response of the FLM is not fast and needs long time to reach the destination point, the rise time of the transient response is 1.1192 seconds and the system takes 2.0359 seconds to reach the settling time as summarized in Table 2 which need to be minimized by improving the system transient response. Because the system transient is slow, the system does not have overshoot. The system response has very small steady state error and can be neglected. Based on this analysis of the system closed loop response without a controller, the concern now is to improve the system transient response to reach the destination point in shorter time. The FLM closed loop response without a controller helps to notice the improvement of the system by the proposed controller and can clearly evaluate the effectiveness of the controller.

It is clearly shown that the tip vibration of the FLM is not large as the largest peak to peak amplitude is 0.06129 radian as demonstrated in Fig. 5 by the red line. The tip vibration is also eliminated in 0.6 seconds which is not a long time. The reason of not generating large amplitude of the tip vibration is because the system closed loop response is very slow and normally the faster response of the system generates larger tip vibration amplitude unless the system is controlled by a robust controller which has the ability to improve the PT response and repress the tip vibration.

4.2 P-H∞ Integrated Controller for FLM system

The *P-H*∞ integrated controller is used to control the FLM system and tested using step input, trajectory input and under disturbance. The results of the proposed controller with the different references are discussed in detail.

4.2.1 Controller Performance with Step Input

The proposed *P-H*∞ integrated controller performance is shown in Fig. 6 using step input reference. The PT response is presented by the dash-dot blue line which demonstrates faster response in terms of the rise and settling time and also has no over shoot and steady state error. The performance shown by the proposed controller is perfect for the PT and has noticeable improvement compared to the closed loop response. Furthermore, the proposed *P-H*∞ integrated controller has a remarkable improvement in the PT of the FLM compared to the performance of the LQR controller which has been studied in [32] and plotted in Fig. 6 for the comparison purpose. The noticeable improvement of the proposed *P-H*∞ integrated controller compared to the closed loop response without controller and the LQR performance explores the large action and influnce of the porposed controller to the FLM system.

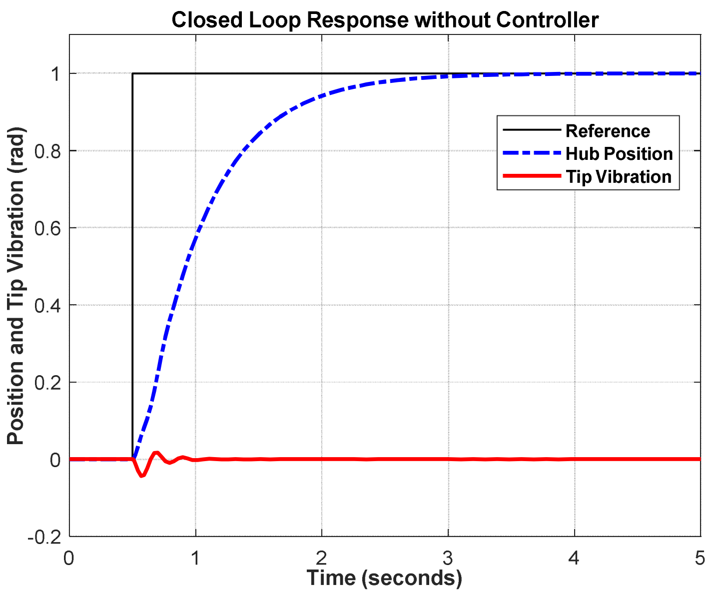

Fig. 5. Closed loop response without controller

Table 4. Analysis of transient response of $P\text{-}H_\infty$ integrated controller

Controller	$T_r(s)$	$T_s(s)$	OS(%)	$e_{ss}(rad)$
$P\text{-}H_\infty$	0.00	0.00	0.00	0.00
LQR [32]	0.1746	0.273	2.74	0.00

Table 5. Analysis of tip VS analysis of $P\text{-}H_\infty$ integrated controller with step input

Controller	Largest peak to peak (rad)	Stable Time (s)
$P\text{-}H_\infty$	0.0608	0.5
LQR [32]	0.5366	0.7

The VS of the $P\text{-}H_\infty$ integrated controller is presented by the solid red line in Fig. 6. The proposed controller is effective to suppress the tip vibration of the FLM as the largest peak to peak amplitude is only 0.0608 radian and can eliminate the vibration in 0.5 seconds. Usualy, the faster response of the PT generates larger amplitude of the tip vibration and takes long time to be eliminated. However, the proposed controller has faster PT reponse and smaller amplitude of the tip vibration compared to the closed loop response of the system without a controller and also the LQR controller. Based on this analysis, the proposed $P\text{-}H_\infty$ integrated controller is optimized for PT and effective for VS of the FLM system as it has better performance than the performance of the LQR controller and the system closed loop response without a controller as well.

4.2.2 Controller Performance with Trajectory Input

The trajectory input is used with three pulses to evaluate the capability of the proposed $P\text{-}H_\infty$ integrated controller for PT and VS. The step input reference is point to point movement and it is easier to be controlled. Thus, using trajectory input reference will better explore the capability of the proposed controller. Based on the controller performance shown in Fig. 7, the proposed $P\text{-}H_\infty$ integrated controller has the ability to efficiently track the trajectory reference. The amplitude of the second and third pulses is double the first pulse, so they generate larger amplitude of the tip vibration as demonstrated in Fig. 7 and summarized in Table 6. Despite the amplitudes of the tip vibration that caused by the second and third pulses are double larger than the amplitude of the tip vibration that generated by the fist pulse, the proposed $P\text{-}H_\infty$ integrated controller eliminates them in reasonable time 0.7 seconds. Overall, the performance of the controller in this case is satisfactory in both PT and VS.

4.2.3 Controller Performance with Disturbance

Any unexpected external force which negatively affects the system output is defined as a disturbance. A robust controller should have the capability to reject disturbances' effects to the system performance. In this case, the tip of the FLM is suddenly displaced 0.4 radian in order to test the robustness of the proposed $P\text{-}H_\infty$ integrated controller. The robustness of the proposed controller is evaluated by the robustness index, the smaller value of the robustness index the higher robust controller. The robustness index is calculated based on the root mean square error (RMSE) which is explained in details in [33]. The robustness index value of the position tacking for the proposed $P\text{-}H_\infty$ integrated controller as in Table 7 is zero which indicates the high robustness of the controller. It means that the sudden displacement of the tip of the FLM does not displace the hub position. Based on the performance of the proposed $P\text{-}H_\infty$ integrated controller shown in Fig. 8 and Table 8, the proposed controller has good robustness to reject the disturbance and to eliminate the tip vibration caused by the external disturbance. Even the tip of the FLM is suddenly displaced 0.4 radian, which is a large displacement, the $P\text{-}H_\infty$ integrated controller keeps the stability of the hub PT without any displacement caused by the disturbance which is perfect behavior of the controller. This performance of the proposed $P\text{-}H_\infty$ integrated controller in the presence of the disturbance shows high robustness to reject the disturbance and to keep the system in its stable situation.

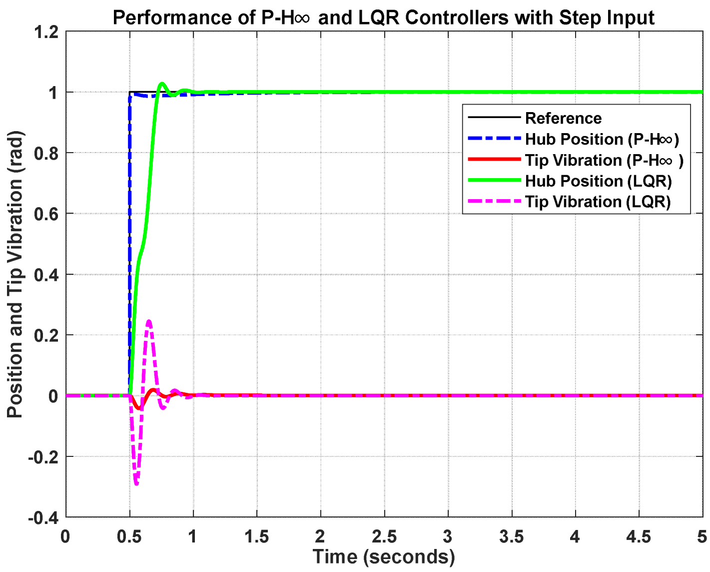

Fig. 6. The $P\text{-}H_\infty$ integrated controller performance with step input compared to the performance of LQR controller from the study in [32].

Table 6. Analysis of tip VS analysis of P-H_∞ integrated controller with trajectory input

	Largest peak to peak (rad)	Stable Time (s)
First pulse	0.0608	0.5
Second pulse	0.1216	0.7
Third pulse	0.1216	0.7

Table 7. Robustness analysis of the P-H_∞ integrated controller under disturbance

System status	RMSE	Robustness index
No disturbance	0.0021	0
With disturbance	0.0021	

Table 8. Analysis of tip VS analysis of P-H_∞ integrated controller under disturbance

Largest peak to peak (rad)	Stable Time (s)
0.02218	0.4

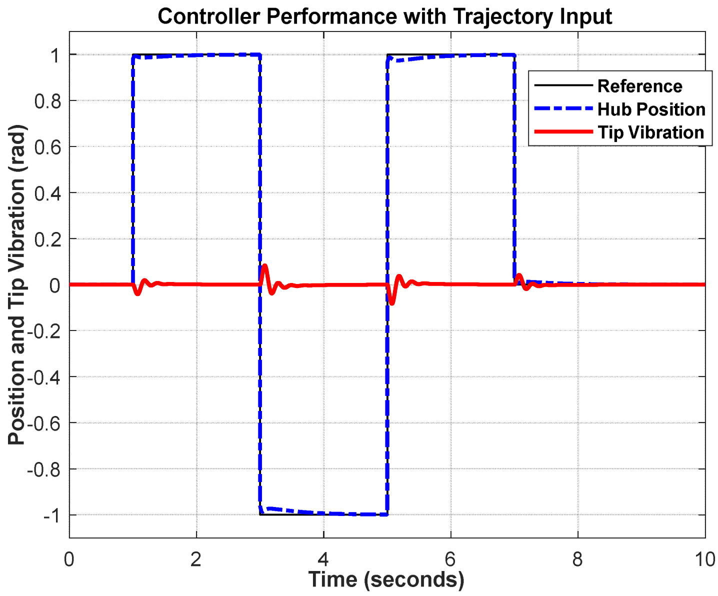

Fig. 7. The P-H_∞ integrated controller performance with trajectory input

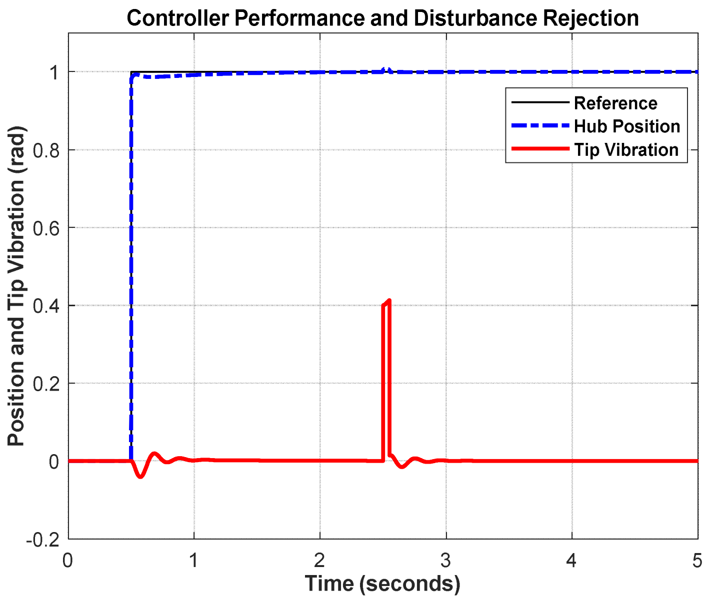

Fig. 8. The P-H_∞ integrated controller performance in the presence of disturbance

5. Conclusion

FLMs has received high concern in research due to their features over traditional manipulators. Thus, this research has proposed the robust P-H_∞ integrated controller to control the FLM system in terms of PT and to overcome the less position accuracy caused by the tip vibration. The proposed P-H_∞ integrated controller is evaluated to control the FLM system using step input and trajectory input. The proposed controller is also tested for its robustness by applying external disturbance to the tip of the FLM. In terms of PT, the proposed P-H_∞ integrated controller has shown satisfactory PT either for the step input and the trajectory reference input. It has also demonstrated high effectiveness of VS. Furthermore, the proposed controller has high robustness based on its explored capability to reject the disturbance. The proposed controller has satisfactorily performed for PT, VS, and disturbance rejection in simulation environment using the MATLAB/Simulink toolbox. However, the experimental validation will be carried out in future work which is better for the validation of the proposed controller for PT, VS, and disturbance rejection.

Author Contributions

Esmail Ali Alandoli suggested the idea, initiated the control design, and wrote the manuscript draft; T. S. Lee participated in the idea improvement, helped in the control design and analysis; Chu A My participated in the control design and analysis; Marwan Qaid Mohammed participated in the control design and analysis. The results, the contribution and the final version of the manuscript are revised and approved by all authors.

Acknowledgments

The authors acknowledge the support of Multimedia University through MMU GRA Scheme (MMUI/180265) and they would like to dedicate sincere thanks to Multimedia University.

Conflict of Interest

The authors declared no potential conflicts of interest with respect to the research, authorship, and publication of this article.

References

[1] Sayahkarajy, M., Mohamed, Z., Mixed sensitivity H_2/H_∞ control of a flexible-link robotic arm, *International Journal of Mechanical and Mechatronics Engineering*, 14(1), 2014, 21-27.

[2] My, C. A., Bien, D. X., Hieu, C., Packianather, M., An efficient finite element formulation of dynamics for a flexible robot with different type of joints, *Mechanism and Machine Theory*, 134, 2019, 267–288.

[3] Dixit, R., Kumar, R.P., Working and limitations of cable stiffening in flexible link manipulators, *Advances in Acoustics and Vibration*, 2016, 2016, 1–9.

[4] Zebin, T., Alam, M.S., Dynamic modeling and fuzzy logic control of a two-link flexible manipulator using genetic optimization techniques, In: *Proceedings of the 13th International Conference on Computer and Information Technology (ICCIT)*, Dhaka, Bangladesh, 418-423, 2010.

[5] My, C. A., Bien, D. X., New development of the dynamic modeling and the inverse dynamic analysis for flexible robot, *International Journal of Advanced Robotic Systems*, 17(4), 2020, 1–12.

[6] Geniele, H., Patel, R.V., Khorasani, K., End-point control of a flexible-link manipulator: theory and experiments, *IEEE Transactions on Control Systems Technology*, 5(6), 1997, 556-570.

[7] Khairudin, M., Mohamed, Z., Husain, A.R., Dynamic model and robust control of flexible link robot manipulator, *Telkomnika*, 9(2), 2011, 279–287.

[8] Raouf, F., Mohamad, S., Maarouf, S., Maamar, B., Distributed adaptive control strategy for flexible link manipulators, *Robotica*, 35(7), 2017, 1562-1584.

[9] Suklabaidya, S., Lochan, K., Roy, B.K., Control of rotational base single link flexible manipulator using different SMC techniques for variable payloads. In: *Proceedings of IEEE International Conference on Energy, Power and Environment: Towards Sustainable Growth (ICEPE)*, Shillong, India 1-6, 2015.

[10] Shawky, A., Zydek, D., Elhalwagy, Y.Z., Ordys, A., Modeling and nonlinear control of a flexible-link manipulator, *Applied Mathematical Modelling*, 37(23), 2013, 9591-9602.

[11] Bien, D.X., My, C.A., Khoi, P.B., Dynamic analysis of two-link flexible manipulator considering the link length ratio and the payload, *Vietnam Journal of Mechanics*, 39(4), 2017, 303-313.

[12] Bien, D. X., My, C. A., Khoi, P. B., Dynamic modeling and control of a flexible link manipulators with translational and rotational joints, *VNU Journal of Science: Mathematics-Physics*, 34(1), 2018, 52-66.

[13] San-Millan, A., Feliu, V., Garcia, A., A two-stage control scheme of single-link flexible manipulators, In: *Proceedings of IEEE 23rd Mediterranean Conference on Control and Automation (MED)*, Torremolinos, Spain, 1098-1105, 2015.

[14] Akyüz, I.H., Kizir, S., Bingül, Z., Fuzzy logic control of single-link flexible joint manipulator, In: *Proceedings of the IEEE International Conference on Industrial Technology*, Auburn, AL, USA, 306-311, 2011.

[15] Akyuz, I.H., Yolacan, E., Ertunc, H.M., Bingul, Z., PID and state feedback control of a single-link flexible joint robot manipulator, In: *Proceedings of the IEEE International Conference on Mechatronics*, Istanbul, Turkey, 409-414, 2011.

[16] Pedro, J.O., Tshabalala, T., Hybrid NNMPC/PID control of a two-link flexible manipulator with actuator dynamics, In: *Proceedings of the 10th IEEE Asian Control Conference (ASCC)*, Kota Kinabalu, Malaysia, 1-6, 2015.

[17] Mahamood, R.M., Pedro, J.O., Hybrid PD/PID controller design for two-link flexible manipulators, In: *Proceedings of the 8th IEEE Asian Control Conference (ASCC)*, Kaohsiung, Taiwan, 1358-1363, 2011.

[18] Khorasgani, H.G., Ghiasi, N.E., Farshad, A., Talebi, H.A., Nonlinear robust control of flexible-link manipulator with fuzzy compensator: experimental results, In: *Proceedings of the 2nd IEEE International Conference on Control, Instrumentation and Automation*, Shiraz, Iran, 993-998, 2011.

[19] Kasdirin, H. A., Assemgul, M., Tokhi, M. O., Fuzzy logic based controller for a single-link flexible manipulator using modified invasive weed optimization, In: *Proceedings of IEEE International Conference on Evolving and Adaptive Intelligent Systems (EAIS)*, Douai, France, 1–6, 2015.

[20] Lu, E., Li, W., Yang, X., Fan, M., Liu, Y., Modelling and composite control of single flexible manipulators with piezoelectric actuators, *Shock and Vibration*, 2016, 2016. 1–14.

[21] Qingsong, C., Ailan, Y., Optimal actuator placement for vibration control of two-link piezoelectric flexible manipulator, In: *Proceedings of the IEEE International Conference on Mechanic Automation and Control Engineering*, Wuhan, China, 2448-2451, 2010.

[22] Hassan, M., Dubay, R., Li, C., Wang, R., Active vibration control of a flexible one-link manipulator using a multivariable predictive controller, *Mechatronics*, 17(6), 2007, 311–323.

[23] Jodouin, P., Saad, M., Wamkeue, R., Linear control of a flexible arm system: Comparison of H_∞ and loop transfer recover methods-application to an experimental arm, In: *Proceedings of the 17th IEEE Mediterranean Electrotechnical Conference*, Beirut, Lebanon, 310-314, 2014.

[24] Axelsson, P., Helmersson, A., Norrlöf, M., H_∞ controller design methods applied to one joint of a flexible industrial manipulator, *IFAC Proceedings Volumes*, 47(3), 2014, 210-216.

[25] Ahmad, M. A., Vibration and input tracking control of flexible manipulator using LQR with non-collocated PID controller, In: *Proceedings of the Second UKSIM European Symposium on Computer Modeling and Simulation*, Liverpool, UK, 40–45, 2008.

[26] Baroudi, M., Saad, M., W. Ghie., State-Feedback and Linear Quadratic Regulator Applied to a Single-Link Flexible Manipulator, In: *Proceedings of the IEEE International Conference on Robotics and Biomimetics (ROBIO)*, Guilin, China, 1381–1386, 2009.

[27] Kherraz, K., Hamerlain, M., Achour, N., Robust sliding mode controller for a class of under-actuated systems, In: *Proceedings of the 15th IEEE International Conference on Sciences and Techniques of Automatic Control and Computer Engineering*, Hammamet, Tunisia, 942-946, 2014.
[28] Lee, T. S., Alandoli, E. A., A critical review of modelling methods for flexible and rigid link manipulators, *Journal of the Brazilian Society of Mechanical Sciences and Engineering*, 42(10), 2020, 508.
[29] Alandoli, E. A., Lee, T. S., A Critical Review of Control Techniques for Flexible and Rigid Link Manipulators, *Robotica*, 38(12), 2020, 2239-2265.
[30] Fareh, R., Saad, M., Saad, M., Distributed control strategy for flexible link manipulators, *Robotica*, 33(4), 2015, 768-786.
[31] Altıner, B., Delibaşı, A., Erol, B., Modeling and control of flexible link manipulators for unmodeled dynamics effect, *Proceedings of the Institution of Mechanical Engineers, Part I: Journal of Systems and Control Engineering*, 233(3), 2019, 245-263.
[32] Alandoli, E. A., Rashid, M. Z. A., Sulaiman, M., A comparison of PID and LQR controllers for position tracking and vibration suppression of flexible link manipulator, *Journal of Theoretical and Applied Information Technology*, 95(13), 2017, 2949–2955.
[33] Alandoli, E. A., Sulaiman, M., Rashid, M. Z. A., Robustness and Disturbance Rejection of *PD/H-*$_\infty$ Integrated Controller for Flexible Link Manipulator System, *Journal of Engineering Science and Technology Review*, 12(1), 2019, 27–36.
[34] Alandoli, E. A., Shah, H. N. M., Sulaiman, M., Rashid, M. Z. A., Aras, M. S. M., *PD/H-*$_\infty$ Integrated Controller for Position Tracking and Vibration Suppression of Flexible Link Manipulator System, *International Journal of Mechanical and Mechatronics Engineering*, 18(3), 2018, 54-61.
[35] Rijanto, E., Standard *H-*$_\infty$ Controller: *Robust Control Theory for Application from* H_2 *to mixed* $H_2/H_{-\infty}$ *control*, ITB Press, Indonesia, 2000.

ORCID iD

Esmail Ali Alandoli https://orcid.org/0000-0002-1132-6095
Chu A. My https://orcid.org/0000-0002-8359-2042
Marwan Qaid Mohammed https://orcid.org/0000-0001-9734-6267

How to cite this article: Alandoli E.A., Lee T.S., My C.A., Mohammed M.Q. Robust P-H$_\infty$ Integrated Controller for Flexible Link Manipulator System in the Presence of Disturbance, *J. Appl. Comput. Mech.*, 7(2), 2021, 646–654. https://doi.org/10.22055/JACM.2020.35475.2668